Desalination and Water Treatment
www.deswater.com
doi: 10.5004/dwt.2020.25446

190 (2020) 125–134
June

Effect of reaction crystallization process parameters on struvite recovery from animal wastewater in presence of boron, cobalt, manganese and molybdenum

Nina Hutnik[a], Anna Stanclik[a], Krzysztof Piotrowski[b,*]

[a]*Wroclaw University of Science and Technology, Department of Engineering and Technology of Chemical Processes, Wybrzeze Wyspianskiego 27, 50–370 Wroclaw, Poland, Tel./Fax: +(071) 320 40 41; emails: nina.hutnik@pwr.edu.pl (N. Hutnik), anna.stanclik@pwr.edu.pl (A. Stanclik)*
[b]*Silesian University of Technology, Department of Chemical Engineering and Process Design, M. Strzody 7, 44–101 Gliwice, Poland, Tel./Fax: +(032) 237 14 61; email: krzysztof.piotrowski@polsl.pl (K. Piotrowski)*

Received 4 February 2019; Accepted 4 January 2020

ABSTRACT

One of the sources of phosphates(V) is liquid manure where the typical content of phosphorus is 0.2–0.4 mass %. It is usually accompanied by nitrogen (0.45–0.64 mass %), potassium (0.3–0.6 mass %), magnesium (0.1 mass %) and calcium (0.3 mass %). Recovery of phosphate(V) ions in a form of sparingly soluble salts is an extremely complex technological process, where competing for precipitation reactions of magnesium ammonium phosphate(V) hexahydrate (struvite, $MgNH_4PO_4{\cdot}6H_2O$) and calcium phosphates co-run. The research results covering the effects of boron, cobalt, manganese and molybdenum in liquid manure on the recovery of phosphate(V) ions in a form of sparingly soluble salt, struvite, are demonstrated. The largest mean size of struvite crystals corresponded to the presence of boron, whereas the smallest one–the presence of cobalt. Boron and manganese influenced struvite habit (thinner and longer crystals). Depending on feed composition and work parameters of the crystallizer, crystal linear growth rate G of struvite varied from 4.79×10^{-9} to 1.91×10^{-8} m s^{-1}, whereas their nucleation rate B varied from 6.8×10^{6} to 4.6×10^{9} s^{-1} m^{-3}. The largest mean struvite crystal size (L_m 75.5 μm) and acceptable homogeneity of population (CV 68.3%) corresponded to inlet solution containing 0.20 mass % of PO_4^{3-} and 5.0 mg B kg^{-1}, with PO_4^{3-}:Mg^{2+} set as 1:1.2, at pH 9 and for a mean residence time of suspension in a crystallizer τ 3,600 s.

Keywords: Struvite recovery; Phosphate(V) ions; Boron; Cobalt; Manganese; Molybdenum

1. Introduction

One of the sources of phosphates(V) may be liquid manure [1]. Depending on specific origin of such liquid manure (cattle or pig) typical content of phosphorus is 0.2–0.4 mass % (0.6–1.2 mass % as phosphates(V)) [2]. High concentration of phosphorus in liquid manure coexists with high concentrations of nitrogen (0.45–0.64 mass %), potassium (0.3–0.6 mass %), magnesium (0.1 mass %) and calcium (0.3 mass %) [3,4]. Because concentrations of these components are quite similar, selective recovery of phosphate(V) ions in a form of sparingly soluble salts is an extremely complex technological process [2–5]. Some competing co-precipitation reactions of magnesium ammonium phosphate(V) hexahydrate (struvite, $MgNH_4PO_4{\cdot}6H_2O$, MAP) [6] and calcium phosphates co-run in this environment. Amorphous calcium phosphates, $Ca_3(PO_4)_2{\cdot}nH_2O$, ACP or TCP [7] mainly precipitate. Also impurities, micronutrients and iron present in liquid manure influence the process course [2], mainly: boron, cobalt, copper, manganese, molybdenum and zinc compounds [8]. These can catalyze or inhibit co-precipitation of struvite and calcium phosphates, as well as other sparingly soluble salts or/and hydroxides. Such compounds may also influence their

* Corresponding author.

further competitive growth up to the macroscopic size [9]. Reaction crystallization of phosphate salts is also affected by the concentration of phosphate(V) ions in wastewater and pH of mother liquor in a crystallizer [10]. The phosphate(V) to calcium ions ratio at the crystallizer feed is also of primary importance [11,12]. This proportion is mainly responsible for reaction crystallization yield of struvite or/and calcium phosphates ACP [13]. Process kinetics and chemical composition of the product result also from eventual usage of an excess of magnesium ions related to inlet concentrations of phosphate(V) and ammonium ions, as well as from a given residence time of suspension in a crystallizer [14]. All mentioned factors influence the possibilities of application of these products in agriculture [15].

The research results covering the influence of selected, specific elements present naturally in liquid manure (boron, cobalt, manganese and molybdenum) on the technical possibilities of recovery of phosphate(V) ions in a form of sparingly soluble salt, mainly struvite, are presented. The process ran under continuous mode in a draft tube mixed suspension mixed product removal (DT MSMPR) crystallizer [16]. The influence of crystallizer work parameters on the product quality, as well as on nucleation and growth kinetics of struvite crystals–the main component of the solid product–was identified experimentally. Moreover, the individual effect of each impurity was also referred to and compared with the product manufactured based on synthetic liquid manure (SLM) or synthetic animal breeding wastewater (SABW) [17].

2. Experimental

The research tests were carried out in a continuous, fully automated experimental plant (Fig. 1) (IKA, Germany Labortechnik).

Reaction crystallization of $MgNH_4PO_4 \cdot 6H_2O$ ran in a continuous DT MSMPR type crystallizer with an internal circulation of suspension forced by propeller stirrer, of working volume V_w 0.6 dm^3. Mixer speed, process temperature, inlet streams of feed and alkalizing solutions, as well as outlet stream of suspension of product crystals from the crystallizer were precisely controlled and adjusted

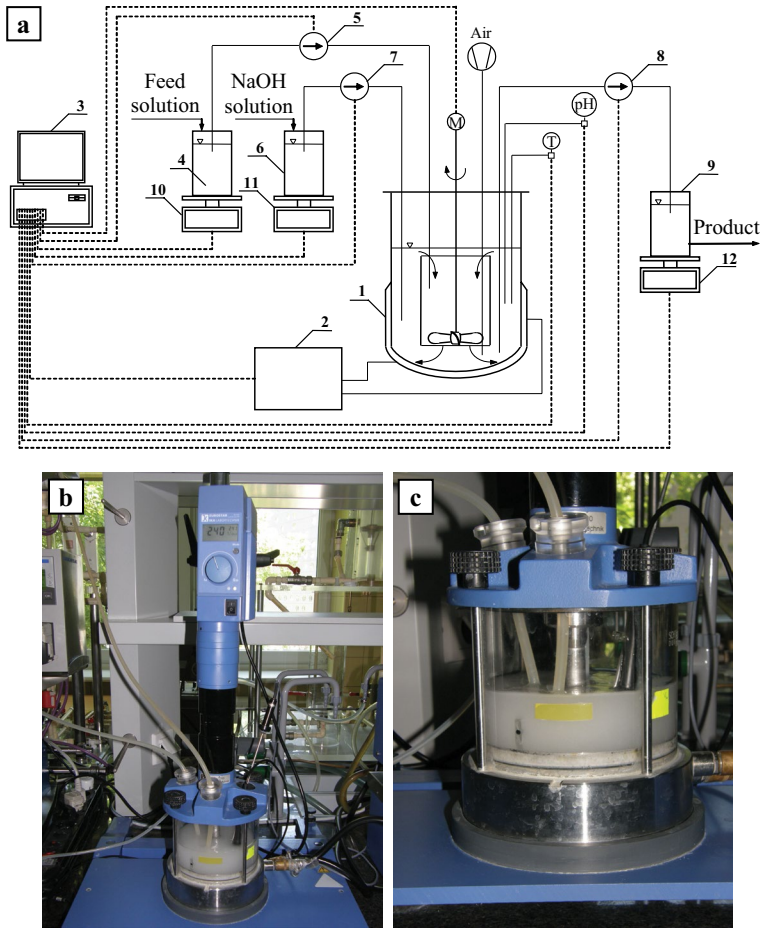

Fig. 1. Schematic diagram of the experimental plant (a) 1–DT MSMPR type crystallizer with an internal circulation of suspension, 2–thermostat, 3–PC computer, 4–feed reservoir: aqueous solution of $MgCl_2 \cdot 6H_2O$, $NH_4H_2PO_4$, and impurities, 5–feed proportioner (pump), 6–alkalinity agent tank: aqueous solution of NaOH, 7–proportioner (pump) of NaOH solution, 8–receiver (pump) of product crystal suspension from the crystallizer tank, 9–storage tank of a product crystal suspension, 10, 11, 12–electronic balances, *M*–stirrer speed control/adjustment, pH–alkaline/acid reaction control/adjustment, *T*–temperature control/adjustment. Photos: (b) general view and (c) plant detail–continuous DT MSMPR crystallizer unit with an internal circulation of suspension.

by PC computer (the software applied: IKA Labworldsoft and BioScadaLab).

Crystallizer feed was represented by an aqueous solution of ammonium dihydrogen phosphate(V) $NH_4H_2PO_4$ and magnesium chloride hexahydrate $MgCl_2{\cdot}6H_2O$, together with the impurities tested. Cobalt and manganese compounds were introduced in a crystalline form–as cobalt chloride hexahydrate $CoCl_2{\cdot}6H_2O$ or/and manganese chloride tetrahydrate $MnCl_2{\cdot}4H_2O$ (p.a. POCh, Gliwice, Poland), whereas boron and molybdenum compounds were provided as the standard solutions of H_3BO_3 or/and $(NH_4)_6Mo_7O_{24}$ (CertiPUR, Merck, Germany). Feed solution of required composition was prepared in an external mixer, provided with deionized water (Barnstead–NANOpure DIamond) and required doses of appropriate chemicals.

Chemical compositions of the feed solutions are presented in Table 1.

Concentrations of impurities were purposefully selected considering their typical ranges in the real liquid manures of various origins [1,2,8]. The feed was then systematically pumped into the crystallizer assuming constant volumetric stream q_v 2.4 or 0.6 dm^3 h^{-1} (resulting in required mean residence time of suspension in a crystallizer $\tau = V_w/q_v$ 900 or 3,600 s, correspondingly). Crystallizer was also provided with precisely and flexibly dosed injections of an aqueous solution of sodium hydroxide, of concentration 20 mass % of NaOH in an amount providing the demanded, controlled pH of the struvite continuous reaction crystallization environment. The research tests ran under stoichiometric conditions (PO_4^{3-}:Mg^{2+}:NH_4^+ as 1:1:1) and with magnesium ions excess (as 1:1.2:1), in temperature 298 K, assuming pH 9 or 11. Crystallizer unit and its work details were presented elsewhere [18]. Determination of product crystal size distribution (CSD) and calculation on this basis population density distribution n(L) with crystal shape estimation (crystal length L_a/crystal width L_b) was also described in other works [14]. Analytical procedures and methods involved, as well as methods of determination of chemical and phase compositions of the products, were described earlier [19]. For this purpose the X-ray fluorescence spectrometer was used, while for the phase identification–the X-ray diffractometer and some thermal analysis methods (DTA, TG, DTG) were applied (Fig. 2).

CSD and population population density distribution n(L) were determined for each product. On this basis the kinetic parameters of struvite continuous reaction crystallization process were estimated. Simplified size-independent growth (SIG) kinetic model of the mass crystallization process in a continuous MSMPR crystallizer was applied [16,20]. Fundamental assumptions of the model, dependencies and formulas involved in the calculations, as well as the method of kinetic parameters interpretation are shown in [14]. According to the SIG MSMPR model assumptions in general population balance, the population density distribution of product crystals is presented in a form of (1):

$$n(L) = n_0 \exp\left(-\frac{L}{G\tau}\right) \tag{1}$$

where $n(L)$ is crystal population density for a given particle size L, n_0 is nuclei population density (n for $L = 0$), L is crystal size, G is a linear growth rate of crystal, τ mean residence time of suspension in a crystallizer.

Linear crystal growth rate G can be computed from the regression analysis fitting the experimental $n(L)$ data with Eq. (1). For the known G and nuclei population density n_0, nucleation rate B can be calculated from Eq. (2):

$$B = n_0 G \tag{2}$$

3. Results and discussion

The effects of characteristic for liquid manure impurities and work parameters of the crystallizer on continuous struvite reaction crystallization process are demonstrated in Table 2. Molar proportions of substrate ions PO_4^{3-}:Mg^{2+}:NH_4^+ in a feed was set as 1:1:1 (stoichiometric conditions). Concentrations of: boron, cobalt, manganese and molybdenum were selected carefully to approach their concentrations in liquid manure SABW (Table 1). The influence of concentration of each impurity on struvite reaction crystallization process was presented in different work of the authors [21]. Every single impurity affected product quality in a different way. For the following process parameters: inlet concentration of phosphate(V) ions $[PO_4^{3-}]_{RM}$ 1.0 mass %, pH 9, τ 900 s

Table 1
Chemical composition of synthetic wastewater solutions

Molar proportions of substrate ions in a feed PO_4^{3-}:Mg^{2+}:NH_4^+	Concentration of:									
	PO_4^{3-}	Mg^{2+}	NH_4^+	B		Co		Mn		Mo
	(mass %)	(mass %)	(mass %)	(mg kg^{-1})		(mg kg^{-1})		(mg kg^{-1})		(mg kg^{-1})
1:1:1	0.20	0.0512	0.0380	5.0	or	0.10	or	15.0	or	0.60
	0.208	0.0530	0.451	1.62	and	0.09	and	19.0	and	0.62*
	1.0	0.256	0.190	5.0	or	0.10	or	15.0	or	0.60
1:1.2:1	0.20	0.0614	0.0380	5.0	or	0.10	or	15.0	or	0.60
	0.208	0.0640	0.451	1.62	and	0.09	and	19.0	and	0.62*
	1.0	0.307	0.190	5.0	or	0.10	or	15.0	or	0.60

*and Ca 1,270; K 1,900; Na 500; Cu 6.35; Fe 2.20; Zn 31.2 (mg kg^{-1}) (synthetic animal breeding wastewater – SABW).

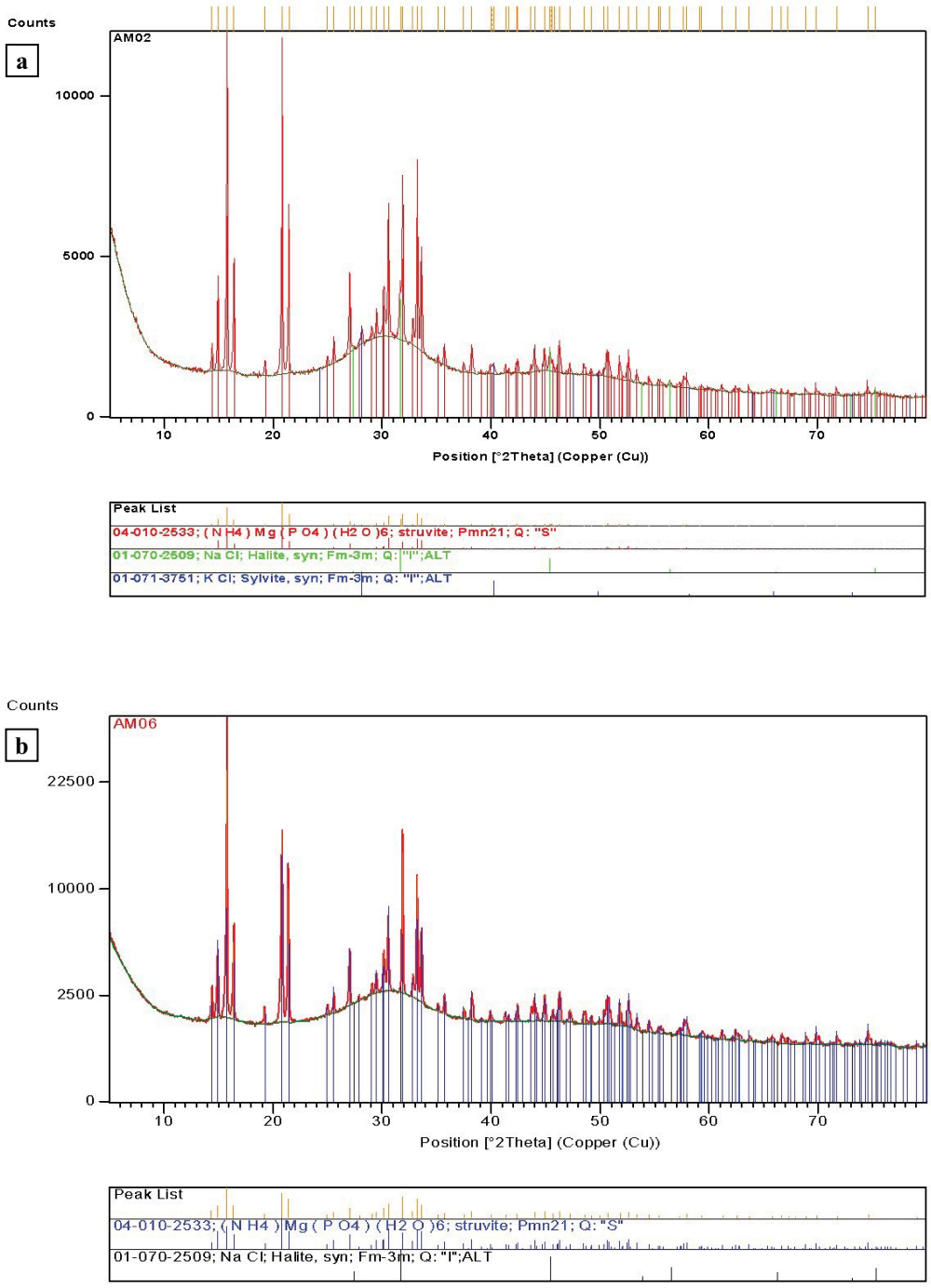

Fig. 2. X-ray diffraction pattern of manufactured product – characteristic peaks of crystalline phases indicate main components of solid phase – struvite and halite. Dominant fraction of the amorphous phase is identified as specific background hump (T 298 K, pH 9, τ 3,600 s, molar ratio of PO_4^{3-}:Mg^{2+} in a feed: (a) 1:1 and (b) 1:1.2).

(tests No. 1, 5, 9 and 13 in Table 2) product of the largest mean crystal size (L_m 40.3 μm) was obtained in presence of boron while representing the smallest size (L_m 27.6 μm) – in presence of cobalt.

These observations are also confirmed by other size distribution parameter of the product, namely median size L_{50}, which was 30.9 μm (for boron) and 21.1 μm (for cobalt), appropriately. The most inhomogeneous product from within the compared distributions (crystal size variation coefficient CV 90.6%) corresponded to the presence of cobalt, while the most homogeneous one (CV 82.0%)–to the presence of molybdenum. Two impurities tested, cobalt and molybdenum, did not practically modify the standard struvite crystals habit (L_a/L_b ca. 6) [9]. Struvite produced in their

presence characterized by L_a/L_b 5.9 and 6.2, appropriately. In the presence of boron these crystals became clearly thinner and longer (L_a/L_b 8.7). Similar changes in geometrical proportions of struvite crystals were observed in the presence of manganese. The effect of manganese presence was not, however, such distinct (L_a/L_b 7.6). One can suppose, that in this case partial blockage of growing struvite crystals surface by co-precipitating manganese hydroxide (534 mg Mn kg^{-1} of the product) occurs. Other impurities were present in a product in small quantities: from 0.1 mg Mo kg^{-1} to 1.3 mg Co kg^{-1} (Table 2). Crystalline product from liquid manure SABW contained as much as 16 520 mg of various impurities kg^{-1} [17]. It should be, however, explained here that the presence of these microelements is not harmful to the plants and even enriches the struvite value as a mineral fertilizer product [2,15].

An increase in environment pH from 9 to 11 resulted in a decrease of struvite crystal sizes and deteriorated the size-homogeneity within their populations. In the presence of cobalt mean size decreased by ca. 30%, while in the presence of boron–by as much as ca. 60%. Non-homogeneity within crystal sizes increased significantly in presence of molybdenum: from CV 82% (pH 9) to CV 126% (pH 11). In the presence of cobalt and manganese increase in CV by ca. 10% was observed, whereas in the presence of boron–by 0.5% only. Since mean crystal size is calculated based on crystal length L_a, shorter L_m at pH 11 produced decrease of L_a/L_b ratio even to 5.2 (in case of molybdenum).

Elongation of the mean residence time of suspension in a crystallizer influenced the final sizes of struvite crystals advantageously. In the presence of cobalt their mean size L_m increased even up to nearly 56 μm, thus more than two-times. In the presence of other impurities increment of L_m from 12% to 20% was noticed. Three impurities tested (boron, manganese and molybdenum) deteriorated the size-homogeneity of struvite crystals. CV for these crystals increased by few (B, Mn) or by a dozen or so % (Mo). Contrary, in the presence of cobalt homogeneity within struvite crystals population clearly improved: CV 90.6% (τ 900 s) decreased advantageously to CV 83.1% (τ 3,600 s) (Table 2). The longer residence time of struvite crystal suspension in a crystallizer established also conditions for their shape modification.

Table 2
Effect of process parameters on the quality of struvite crystals produced from synthetic liquid manure SLM, SABW containing phosphate(V) and: boron, cobalt, manganese or/and molybdenum

No.[c]	Process parameters[a]				Product characteristics[b]				
	Component of SLM, SABW and its inlet concentration	$[PO_4^{3-}]_{RM}$	pH	τ	L_m	L_{50}	CV	L_a/L_b	Impurities
	(mg kg^{-1})	(mass %)	(–)	(s)	(μm)	(μm)	(%)	(–)	(mg kg^{-1})
1	B 5.0	1.0	9	900	40.3	30.9	87.5	8.7	1.1
2		1.0	11	900	15.8	10.7	88.0	6.3	1.2
3		1.0	9	3,600	45.5	34.3	92.1	9.1	1.2
4		0.20	9	3,600	71.1	57.0	76.9	9.3	5.7
5	Co 0.10	1.0	9	900	27.6	21.1	90.6	5.9	1.3
6		1.0	11	900	19.6	13.9	101.0	5.4	1.4
7		1.0	9	3,600	55.9	44.2	83.1	5.2	1.5
8		0.20	9	3,600	59.5	48.0	81.5	5.1	8.0
9	Mn 15.0	1.0	9	900	32.9	25.0	88.9	7.6	534
10		1.0	11	900	15.9	10.4	98.7	6.0	615
11		1.0	9	3,600	39.5	28.4	91.6	7.8	632
12		0.20	9	3,600	57.3	44.2	85.2	7.9	3,010
13	Mo 0.60	1.0	9	900	34.3	27.9	82.0	6.2	0.1
14		1.0	11	900	18.9	10.1	126.0	5.2	0.2
15		1.0	9	3,600	40.1	30.4	94.4	6.1	0.2
16		0.20	9	3,600	67.0	47.2	82.0	6.3	0.5
SABW[d]		0.208	9	3,600	15.5	12.5	76.0	–	16,520

[a] Molar proportions of substrate ions in a feed: PO_4^{3-}:Mg^{2+}:NH_4^+ = 1:1:1.
[b] After drying, without water-washing of solid phase directly on a filter.
Average concentration of phosphate(V) ions in mother liquor: 140 ± 5 mg kg^{-1}.
Solid phase content in a product suspension M_T 23.8 ± 0.4 kg m^{-3} (Tests No. 1–3, 5–7, 9–11, 13–15) and M_T 4.7 ± 0.2 kg m^{-3} (Tests No. 4, 8, 12, 16).
L_m – mean crystal size, $L_m = \Sigma x_i L_i$, where: x_i – mass fraction of crystals of mean fraction size L_i; L_{50} – median crystal size for 50 mass % undersize fraction in cumulative distribution; CV = $100(L_{84} - L_{16})/(2L_{50})$, where: L_{84}, L_{16}, L_{50} – crystal sizes corresponding to: 84, 16 and 50 mass % undersize fractions in cumulative distribution.
[c] Tests No. 1, 5, 9 and 13 [21].
[d] [17].

After a prolonged contact time of supersaturated mother liquor with the crystal phase, the influence of impurities on these crystals habits became more visible. The L_a/L_b ratio for τ 3,600 s was 9.1 (B), 5.2 (Co), 7.8 (Mn) and 6.1 (Mo) (Table 2). As it results from the comparison, the largest deviation from the standard struvite crystals shape was observed in the presence of boron, whereas molybdenum practically did not modify the struvite intrinsic shape.

Decrease of concentration of phosphate(V) ions in a crystallizer feed (from 1.0 to 0.20 mass %) influenced the size distribution of each product advantageously. All distribution parameters improved. The L_m increased by as much as ca. 30 μm on average. The largest value (L_m 71.1 μm) corresponded to the presence of boron. Struvite crystals became more homogeneous. The CV decreased even to below 80% (e.g. in the presence of boron CV 76.9%). Contrary, the content of impurities in solid products increased. For example, providing the crystallizer with manganese in the amount of 15 mg Mn kg^{-1} of the feed resulted in the co-presence of sparingly soluble manganese hydroxide in a product in an amount of 3,010 mg Mn kg^{-1}. Such high content of solid impurities in the products was an effect of five-times lower solid phase content in suspension (M_T 23.8 ± 0.4 kg m^{-3} for $[PO_4^{3-}]_{RM}$ 1.0 mass %, M_T 4.7 ± 0.2 kg m^{-3} for $[PO_4^{3-}]_{RM}$ 0.20 mass %) (Table 2).

The 20% excess of magnesium ions in relation to inlet concentrations of phosphate(V) and ammonium ions (Table 3) influenced struvite size characteristic especially advantageously.

Providing crystallizer with the solution containing 0.20 mass % of phosphate(V) ions under these conditions, at pH 9 and for mean residence time τ 3,600 s, struvite crystals of mean size L_m bigger even by ca. 10 μm (by ca. 9% larger in average) were produced. Also distinct improvement of population homogeneity within each of the compared products was noticed. The CV decreased to values <80% (Co, Mo) and even to <70% (B, Mn). Crystal shape, however, practically did not change. The effect of individual impurities on struvite crystals habit was similar (compare tests No. 4, 8, 12 and 16 in Table 2 with the tests in Table 3). Scanning electron microscope (SEM) images of these crystals are presented in Fig. 3.

Differences not only in size, but also in shape are visible. For comparison, in Fig. 4 some microscope images of solid products manufactured from liquid manure SABW [17] under stoichiometric conditions (L_m 15.5 μm, Table 2) and at magnesium ions excess (L_m 18.1 μm, Table 3) are presented. The product was aggregated. It contained also large amount of impurities (16 520 mg kg^{-1}–Fig. 4a and 13 660 mg kg^{-1}–Fig. 4b), whereas the mean size of struvite crystals was even four-times smaller than L_m of crystals manufactured in presence of individual impurities tested separately (Tables 2 and 3).

Considering the analyzed results one can conclude, that boron selectively limited growth of struvite crystal faces responsible for width (L_b) only, simultaneously favoring the growth of the faces defining its length L_a by some selected face-oriented surface modification affecting complex interactions with growth units from bulk mother solution.

In the presence of manganese and cobalt the available struvite crystal surface was obstructed by co-precipitated manganese hydroxide and cobalt hydroxide. Obstruction of growing crystals surface induced significant tensions and stresses within the struvite crystal structures, modifying their extending conditions according to its intrinsic crystal network template. Analyzing the SEM images, authors identified some fractures, surface cracks and deformed crystals edges, as well as whole untypical tubular crystalline structures (not classical prismatic ones). In the case of cobalt hydroxide rather splitted and shredded edges of struvite crystals were observed clearly, what may be related to spatial relaxation of structural tensions resulting from surface co-crystallization of hydroxide. This produced also some specific fractures and cracks oriented to L_a axis, as well as the occurrence of asymmetric point surface growth defects. However, the global effect of cobalt and cobalt hydroxide on struvite crystals did not produce any noticeable changes in their habit, since L_a/L_b was ca. 6. Instead, these clearly affected the CSD course (inhomogeneous product).

Table 3
Struvite product characteristics and kinetic parameters of continuous reaction crystallization process at the magnesium ions excess in a feed: PO_4^{3-}:Mg^{2+}:NH_4^+ = 1:1.2:1

Component of SLM, SABW and its inlet concentration[a]	Product characteristics[b]				Kinetic parameters[c]		
	L_m	L_{50}	CV	L_a/L_b	n_0[d]	G	B[d]
(mg kg^{-1})	(μm)	(μm)	(%)	(–)	(m^{-1} m^{-3})	(m s^{-1})	(s^{-1} m^{-3})
B 5.0	75.5	63.5	68.3	9.7	1.0×10^{15}	6.84×10^{-9}	6.8×10^{6}
Co 0.10	69.2	59.5	77.5	4.9	5.1×10^{15}	6.68×10^{-9}	3.4×10^{7}
Mn 15.0	64.1	57.4	65.7	8.0	1.1×10^{16}	5.58×10^{-9}	6.4×10^{7}
Mo 0.60	73.8	57.6	78.1	6.4	6.3×10^{14}	7.44×10^{-9}	4.7×10^{7}
SABW[e]	18.1	14.0	82.1	–	–	–	–

[a] Process parameters: $[PO_4^{3-}]_{RM}$ 0.20 mass %, pH 9, τ 3,600 s.
[b] After drying, without water-washing of solid phase directly on a filter.
[c] From SIG MSMPR kinetic model.
[d] for k_v = 1 (crystal shape coefficient, volume-based parameter).
[e] [17]; impurities in a product: 13,660 mg kg^{-1}.

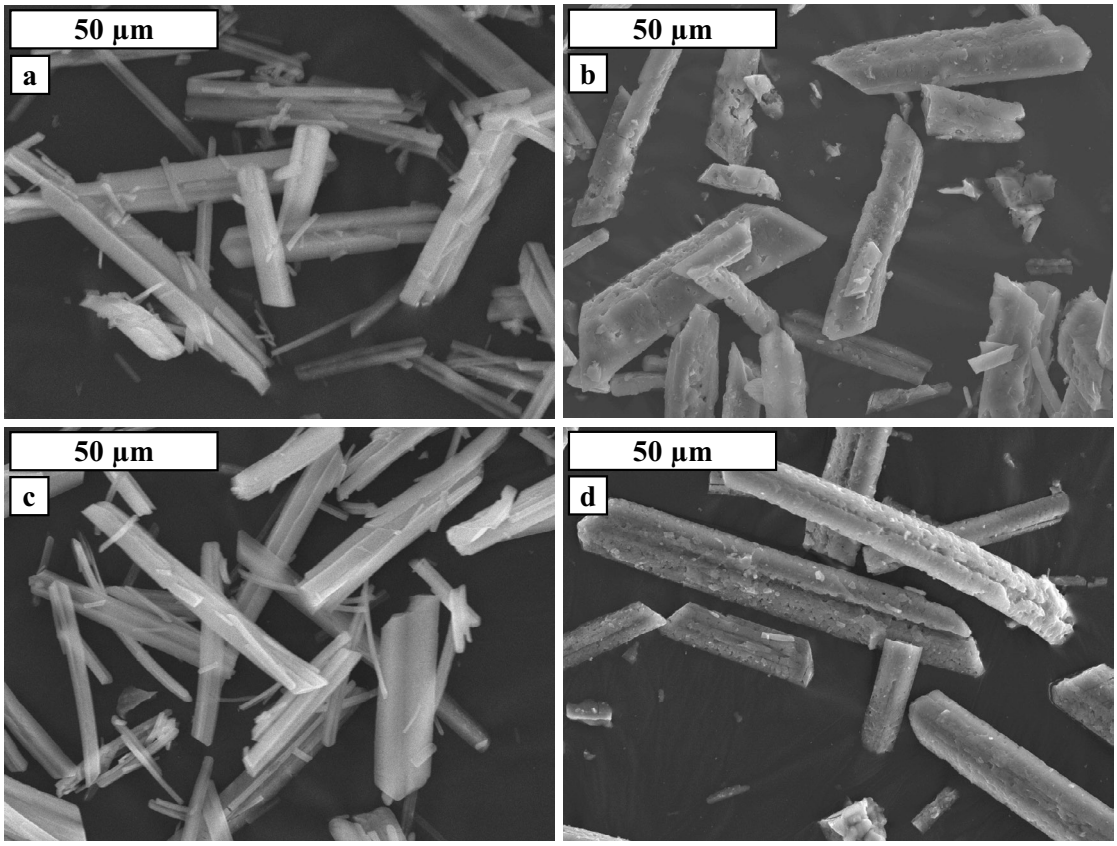

Fig. 3. SEM images of struvite crystals produced in continuous reaction crystallization process in presence of impurities in a feed: (a) B 5.0 mg kg^{-1}, (b) Co 0.10 mg kg^{-1}, (c) Mn 15.0 mg kg^{-1} and (d) Mo 0.60 mg kg^{-1} (for CSD details - Table 3).

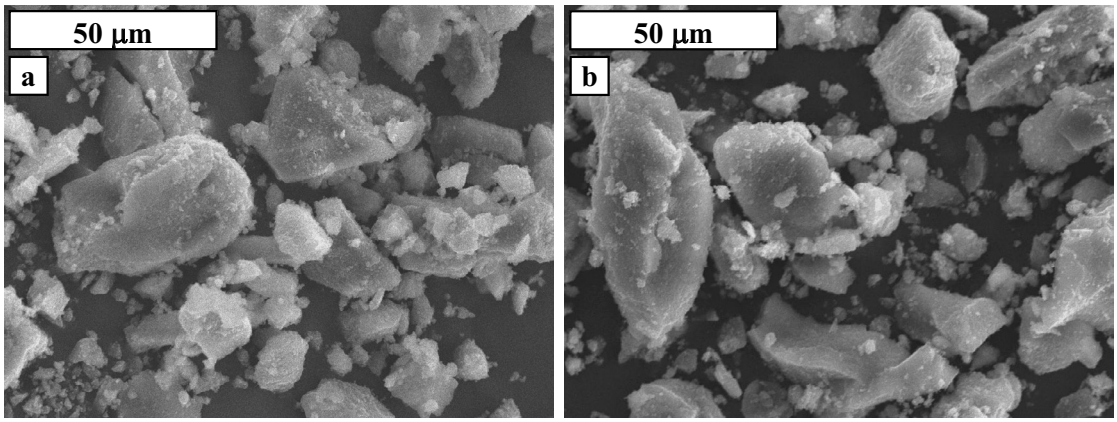

Fig. 4. SEM images of solid products from synthetic liquid manure – SLM, SABW [17]. Molar ratio PO_4^{3-}:Mg^{2+} in a feed: (a) 1:1 and (b) 1:1.2 – Tables 2 and 3 for CSD details.

Contrary, no simultaneous co-precipitation of molybdenum hydroxide under specified process conditions was responsible for relative homogeneity of the population shown as a moderate CV.

Some effects resulting from impurities presence are especially distinctly observable for relatively long mean residence times of suspension in a crystallizer, making prolonged contact between the growing crystal phase and supersaturated mother liquor possible. In such environments longer time available for the modification of mass transfer conditions or even direct taking part in interphase mass transfer produced clearly distinguishable effects in the different product properties (CSD, habit).

Based on mass/volumetric particle size distributions of 20 products manufactured in laboratory conditions (Tables 2 and 3) their numerical distributions were calculated and further transformed into their experimental population density distributions, $n(L)$ (Eq. (1)). The examples (from Table 3) are

presented in Fig. 5. From these ln$n(L)$ distribution courses, it results, that for struvite crystals of size $L > 40$ μm (manufactured in presence of manganese or molybdenum) or $L > 50$ μm (manufactured in presence of boron and cobalt) these dependencies can be satisfactorily approximated with a linear function, as it is predicted by SIG MSMPR kinetic model frame [14].

One can thus calculate linear struvite crystals growth rate G (Eq. (1)) and their nucleation rate B (Eq. (2)). Calculation results are presented in Tables 3 and 4, as well as in Fig. 5.

However, since the kinetic parameters are calculated from a simplified, linear SIG MSMPR model, these should be regarded as the estimated values only [14]. From the analysis of all kinetic data it results, that linear struvite crystals growth rate G varied from 4.79 10^{-9} m s^{-1} (test No. 11 in Table 4) up to 1.91 × 10^{-8} m s^{-1} (test No. 1 in Table 4), whereas nucleation rate B: from 6.8 × 10^{6} s^{-1} m^{-3} (B (boron), Table 3) up to 4.6 × 10^{9} s^{-1} m^{-3} (B (boron), test No. 2 in Table 4). These are large differences, confirming the significant effect of impurities on the processing system and equally important influence of work parameters of continuous crystallizer on continuous struvite reaction crystallization kinetics. The highest linear crystal growth rate of struvite was observed in the presence of boron, G 1.91 × 10^{-8} m s^{-1}, simultaneously observing the lowest nucleation rate, B 2.3 × 10^{8} s^{-1} m^{-3} (test No. 1 in Table 4). The effect of the remaining impurities on struvite crystal growth rate was distinctly smaller: G (1.47–1.51) × 10^{-8} m s^{-1}. Increase in pH of process environment from 9 to 11 produced a decrease of this rate, even to 7.34 × 10^{-9} m s^{-1} (in presence of boron) and to 8.54 × 10^{-9} m s^{-1} (in presence of molybdenum), thus more than two-times (Table 4). The nucleation rate of struvite in the presence of boron was as much as 4.6 × 10^{9} s^{-1} m^{-3}, and nuclei population density n_0 reached the highest value from within all compared cases: 6.3 × 10^{17} m^{-1} m^{-3}. All these together made, that products of unsatisfactory quality (small and inhomogeneous crystals, L_m <20 μm) were manufactured. Decrease of linear struvite crystals growth rate

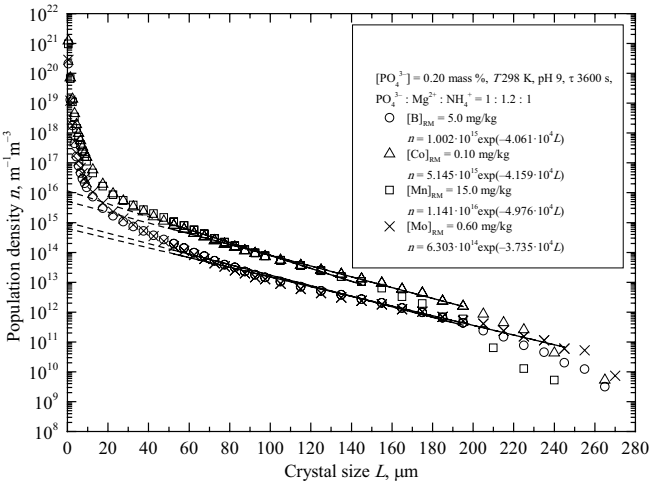

Fig. 5. Effect of impurities present in continuous struvite reaction crystallization process environment on population density distributions of product crystals: points–experimental data, solid straight lines – the $n(L)$ values calculated with Eq. (1)–SIG MSMPR linear kinetic model – fitted to experimental data, valid for crystals fraction $L > 40$ micrometers (Mn, Mo) or $L > 50$ micrometers (B, Co), dashed lines – linear extrapolations of linear SIG MSMPR model (product characteristics – Table 3).

Table 4
Nucleation rate B and linear crystal growth rate G of struvite estimated for continuous reaction crystallization process in DT MSMPR crystallizer. Kinetic parameters calculated with the SIG MSMPR model. Corresponding process conditions (Table 1 and 2)

No.	Component of SLM and its inlet concentration	Kinetic parameters:				
		$n(L)^a$ for $L > 40$ micrometers (Mn, Mo) and $L > 50$ μm (B, Co)	R^2	$n_0{}^a$	G	B^a
			(–)	(m^{-1} m^{-3})	(m s^{-1})	(s^{-1} m^{-3})
1	B 5.0	$n = 1.218 \times 10^{16}\exp(-5.801 \times 10^{4}L)$	0.997	1.2 × 10^{16}	1.91 × 10^{-8}	2.3 × 10^{8}
2		$n = 6.275 \times 10^{17}\exp(-1.514 \times 10^{5}L)$	0.993	6.3 × 10^{17}	7.34 × 10^{-9}	4.6 × 10^{9}
3		$n = 5.877 \times 10^{15}\exp(-4.819 \times 10^{4}L)$	0.989	5.9 × 10^{15}	5.76 × 10^{-9}	3.4 × 10^{7}
4	Co 0.10	$n = 1.366 \times 10^{15}\exp(-4.601 \times 10^{4}L)$	0.980	1.4 × 10^{15}	6.04 × 10^{-9}	8.4 × 10^{6}
5		$n = 2.004 \times 10^{16}\exp(-7.548 \times 10^{4}L)$	0.978	2.0 × 10^{16}	1.47 × 10^{-8}	2.9 × 10^{8}
6		$n = 3.510 \times 10^{16}\exp(-9.916 \times 10^{4}L)$	0.987	3.5 × 10^{16}	1.12 × 10^{-8}	3.9 × 10^{8}
7		$n = 5.868 \times 10^{15}\exp(-4.527 \times 10^{4}L)$	0.994	5.9 × 10^{15}	6.14 × 10^{-9}	3.6 × 10^{7}
8	Mn 15.0	$n = 5.458 \times 10^{15}\exp(-4.386 \times 10^{4}L)$	0.993	5.5 × 10^{15}	6.33 × 10^{-9}	3.5 × 10^{7}
9		$n = 3.479 \times 10^{16}\exp(-7.471 \times 10^{4}L)$	0.995	3.5 × 10^{16}	1.49 × 10^{-8}	5.2 × 10^{8}
10		$n = 8.648 \times 10^{16}\exp(-1.197 \times 10^{5}L)$	0.987	8.6 × 10^{16}	9.28 × 10^{-9}	8.0 × 10^{8}
11		$n = 1.121 \times 10^{16}\exp(-5.796 \times 10^{4}L)$	0.986	1.1 × 10^{16}	4.79 × 10^{-9}	5.2 × 10^{7}
12	Mo 0.60	$n = 7.174 \times 10^{15}\exp(-4.837 \times 10^{4}L)$	0.976	7.2 × 10^{15}	5.74 × 10^{-9}	4.1 × 10^{7}
13		$n = 3.440 \times 10^{16}\exp(-7.333 \times 10^{4}L)$	0.994	3.4 × 10^{16}	1.51 × 10^{-8}	5.1 × 10^{8}
14		$n = 2.149 \times 10^{17}\exp(-1.302 \times 10^{4}L)$	0.974	2.1 × 10^{17}	8.54 × 10^{-9}	1.8 × 10^{9}
15		$n = 9.086 \times 10^{15}\exp(-5.460 \times 10^{4}L)$	0.994	9.1 × 10^{15}	5.09 × 10^{-9}	4.6 × 10^{7}
16		$n = 2.095 \times 10^{15}\exp(-3.502 \times 10^{4}L)$	0.985	2.1 × 10^{15}	7.93 × 10^{-9}	1.7 × 10^{7}

[a] for $k_v = 1$.

G resulted also from elongation of the mean residence time of suspension in a crystallizer, from 900 to 3,600 s (Table 4). In this case, however, the nucleation rate decreased as much as nine-times on average, whereas growth rate *G* decreased ca. three-times only. In the result of reduced (ca. nine-times) nucleation rate (but only ca. three-times smaller crystals growth rate) and advantageously longer (four-times) contact time of growing crystal phase with supersaturated mother liquor, product quality improved distinctly (Table 2).

Lower concentration of phosphate(V) ions in a feed (0.20 mass %) and 20% magnesium ions excess in a process system influenced the struvite continuous reaction crystallization kinetics advantageously. In both cases crystal growth rate increased (Tables 3 and 4). In a result mean crystal size of struvite enlarged up to a maximal value of 71.1 μm under stoichiometric conditions (Table 2) and to 75.5 μm at magnesium ions excess (Table 3). These data concern continuous reaction crystallization of struvite in the presence of boron. The smallest increment of L_m was up to 57.3 and 64.1 μm, respectively, observed in the presence of manganese.

4. Conclusions

The phosphate(V) ions were recovered in a continuous struvite reaction crystallization process from aqueous solutions of wastewaters containing also impurities specific for liquid manure: boron, cobalt, manganese or/and molybdenum. It was generally concluded, that each impurity influenced product quality, nucleation rate and crystals growth rate of struvite–the main component of these products–in a different way. Product of the largest mean size was manufactured in the presence of boron, whereas representing the smallest size–in the presence of cobalt. Boron and manganese influenced struvite crystals habit, making crystals thinner and longer. Raise of pH in a crystallizer from 9 to 11 resulted in the reduction of struvite crystal sizes (even by 60% in the presence of boron) and devaluation of their homogeneity (CV even above 100%). Contrary, elongation of the residence time of suspension in a crystallizer influenced final crystal sizes advantageously. Their mean size in the presence of cobalt enlarged by more than two-times. Reduction of inlet concentration of phosphate(V) ions (from 1.0 to 0.20 mass %) and 20% excess of magnesium ions in relation to concentrations of phosphate(V) and ammonium ions resulted in improvement of size characteristics of the products (larger mean size of crystals by ca. 10 μm, improvement of population homogeneity–CV smaller than 70%).

Kinetic parameters of continuous struvite reaction crystallization process were estimated from SIG MSMPR kinetic model. It was concluded, that depending on crystallizer feed composition and parameters of the crystallizer work, linear crystals growth rate *G* of struvite varied from 4.79×10^{-9} to 1.91×10^{-8} m s^{-1}, whereas nucleation rate *B* from 6.8×10^{6} to 4.6×10^{9} s^{-1} m^{-3}. These are large differences, confirming the significant influence of the investigated impurities–individually and together–and parameters of continuous struvite reaction crystallization process on the quality of the corresponding product. Product representing the largest mean crystal size (L_m 75.5 μm) and of acceptable homogeneity (CV 68.3%) was manufactured from inlet solution containing 0.20 mass % of PO_4^{3-} and 5.0 mg B kg^{-1}, with the assumed molar ratio of PO_4^{3-}:Mg^{2+} set as 1:1.2, at pH 9 and for a mean residence time of suspension in a crystallizer τ 3,600 s. Kinetic parameters of continuous struvite reaction crystallization process under these, the most advantageous conditions, were: *B* 6.8×10^{6} s^{-1} m^{-3} and *G* 6.84×10^{-9} m s^{-1}.

Acknowledgement

The work was supported by the National Science Center of Poland under grant No 2016/21/D/ST8/01694, 2017–2020.

Symbols

ACP	—	Amorphous calcium phosphate, $Ca_3(PO_4)_2$
B	—	Nucleation rate, s^{-1} m^{-3}
CSD	—	Crystal size distribution
CV	—	Coefficient of (crystal size) variation, %
DT	—	Draft Tube
G	—	Linear growth rate of crystal, m s^{-1}
k_v	—	Shape coefficient of a crystal (volume based), –
L	—	Crystal size, μm
L_a	—	Crystal length, μm
L_b	—	Crystal width, μm
L_m	—	Mean crystal size, μm
L_{16}	—	Crystal size corresponding to 16 mass % undersize fraction, μm
L_{50}	—	Median crystal size, μm
L_{84}	—	Crystal size corresponding to 84 mass % undersize fraction, μm
MAP	—	Magnesium ammonium phosphate(V) hexahydrate, struvite
MSMPR	—	Mixed suspension mixed product removal (crystallizer)
M_T	—	Solid phase content in a product suspension, kg_{solid} m^{-3}
n	—	Population density, m^{-1} m^{-3}
n_0	—	Nuclei population density, m^{-1} m^{-3}
$[PO_4^{3-}]$	—	Concentration of phosphate(V) ions, mass %
q_v	—	Volumetric stream, dm^3 h^{-1}
SABW	—	Synthetic animal breeding wastewater
SEM	—	Scanning electron microscopy
SIG	—	Size-independent growth (kinetic model)
SLM	—	Synthetic liquid manure
T	—	Temperature, K
TCP	—	Tricalcium phosphate, $Ca_3(PO_4)_2$
V_w	—	Working volume of the crystallizer, dm^3
x_i	—	Mass fraction of crystals of mean fraction size L_i, –

Greek

τ	—	Mean residence time of suspension in a crystallizer, s

Subscripts

0	—	Related to nuclei
m	—	Mean
RM	—	Raw materials (substrates)
V	—	Volumetric
w	—	Working

References

[1] S.G. Sommer, M.L. Christensen, T. Schmidt, L.S. Jensen, Eds., Animal Manure Recycling, Treatment and Management, Wiley, New Delhi, 2013.

[2] M.M. Rahman, M.A.M. Salleh, U. Rashid, A. Ahsan, M.M. Hossain, C.S. Ra, Production of slow release crystal fertilizer from wastewaters through struvite crystallization – a review, Arabian J. Chem., 7 (2014) 139–155.

[3] Y.H. Liu, J.H. Kwag, J.H. Kim, S.C. Ra, Recovery of nitrogen and phosphorus by struvite crystallization from swine wastewater, Desalination, 277 (2011) 364–369.

[4] M.M. Rahman, Y.H. Liu, J.H. Kwag, S.C. Ra, Recovery of struvite from animal wastewater and its nutrient leaching loss in soil, J. Hazard. Mater., 186 (2011) 2026–2030.

[5] B. Tansel, G. Lunn, O. Mouje, Struvite formation and decomposition characteristics for ammonia and phosphorus recovery, Chemosphere, 194 (2018) 504–514.

[6] S.A. Parsons, Phosphate precipitation from waste waters–recent scientific and technical developments: struvite (magnesium ammonium phosphates), CEEP Scope Newsl., 41 (2001) 15–22.

[7] E. Valsami-Jones, Phosphate precipitation from waste waters–recent scientific and technical developments: calcium phosphate precipitation, CEEP Scope Newsl., 41 (2001) 8–15.

[8] A. Kozik, N. Hutnik, K. Hoffmann, M. Huculak–Maczka, Phosphates(V) ions recovery from cattle manure, Przem. Chem., 94 (2015) 938–942.

[9] K.S. Le Corre, E. Valsami-Jones, P. Hobbs, S.A. Parsons, Phosphorus recovery from wastewater by struvite crystallization: a review, Crit. Rev. Env. Sci. Technol., 39 (2009) 433–477.

[10] A. Kozik, A. Matynia, N. Hutnik, K. Piotrowski, Effect of technological input parameters on struvite separation in a continuous laboratory plant, Przem. Chem., 92 (2013) 796–801.

[11] K.S. Le Corre, E. Valsami-Jones, P. Hobbs, S.A. Parsons, Impact of calcium on struvite crystal size, shape and purity, J. Cryst. Growth, 283 (2005) 514–522.

[12] N. Hutnik, K. Piotrowski, B. Wierzbowska, A. Matynia, Continuous reaction crystallization of struvite from phosphate(V) solutions containing calcium ions, Cryst. Res. Technol., 46 (2011) 443–449.

[13] N. Hutnik, A. Stanclik, A. Matynia, Influence of calcium ions on struvite precipitation and crystallization from wastewaters, Przem. Chem., 96 (2017) 1864–1868.

[14] A. Kozik, N. Hutnik, K. Piotrowski, A. Matynia, Continuous reaction crystallization of struvite from diluted aqueous solution of phosphate(V) ions in the presence of magnesium ions excess, Chem. Eng. Res. Des., 92 (2014) 481–490.

[15] M. Latifian, J. Liu, B. Mattiasson, Struvite-based fertilizer and its physical and chemical properties, Environ. Technol., 33 (2012) 2691–2697.

[16] J.W. Mullin, Crystallization, Butterworth-Heinemann, Oxford, 1993.

[17] A. Kozik, N. Hutnik, B. Wierzbowska, K. Piotrowski, A. Matynia, Recovery of struvite from synthetic animal wastewater by continuous reaction crystallization process, Int. J. Chem. Eng. Appl., 7 (2016) 47–50.

[18] N. Hutnik, A. Kozik, A. Mazienczuk, K. Piotrowski, B. Wierzbowska, A. Matynia, Phosphates(V) recovery from phosphorus mineral fertilizers industry wastewater by continuous struvite reaction crystallization process, Water Res., 47 (2013) 3635–3643.

[19] A. Kozik, N. Hutnik, J. Podwórny, A. Gerle, A. Mazienczuk, A. Matynia, Recovery of phosphate(V) ions from synthetic swine wastewater under stoichiometric conditions, Przem. Chem., 93 (2014) 559–564.

[20] A.D. Randolph, M.A. Larson, Theory of Particulate Processes: Analysis and Techniques of Continuous Crystallization, 2nd ed., Academia Press, New York, 1988.

[21] N. Hutnik, A. Stanclik, K. Piotrowski, Boron, cobalt, manganese and molybdenum compounds in the phosphate recovery from animal wastewater, Przem. Chem., 97 (2018) 294–298.